

Bulge formation in disk galaxies with MOND

F. Combes¹

Observatoire de Paris, LERMA (CNRS:UMR8112), 61 Av. de l'Observatoire, F-75014, Paris, France e-mail: francoise.combes@obspm.fr

Received 2014/ Accepted 2014

ABSTRACT

The formation of galaxies and their various components can be stringent tests of dark matter models and of gravity theories. In the standard cold dark matter (CDM) model, spheroids are formed through mergers in a strongly hierarchical scenario, and also in the early universe through dynamical friction in clumpy galaxies. More secularly, pseudo-bulges are formed by the inner vertical resonance with bars. The high efficiency of bulge formation is in tension with observations in the local universe of a large amount of bulge-less spiral galaxies. In the present work, the formation of bulges in very gas-rich galaxies, as those in the early universe, is studied in the Milgrom's Modified Newtonian Dynamics (MOND), through multi-grid simulations of the non-linear gravity, including the gas dissipation, star formation and feedback. Clumpy disks are rapidly formed, as in their Newtonian equivalent systems. However, the dynamical friction is not as efficient, in the absence of dark matter halos, and the clumps have no time to coalesce into the center to form bulges, before they are eroded by stellar feedback and shear forces. Previous work has established that mergers are less frequent in MOND, and classical bulges are expected less massive. It is now shown that gas-rich clumpy galaxies in the early universe do not form bulges. Since pseudo-bulges are formed with a similar rate as in the Newtonian equivalent systems, it can be expected that the contribution of pseudo-bulges is significantly higher in MOND.

Key words. Galaxies: bulges — Galaxies: evolution — Galaxies: formation — Galaxies: halos — Galaxies: kinematics and dynamics

1. Introduction

Many problems in cosmology, either related to the missing mass in galaxies and clusters, or to the formation of large-scale structures and galaxies, are solved by the existence of a dark sector, dark matter and dark energy, dominating the content of the universe (e.g. Blumenthal et al. 1984, Peebles & Ratra 2003). The standard hypothesis for dark matter is the cold and massive elementary particle (CDM) coming from supersymmetry (Bertone et al 2005), although there is also a recent revival of warm dark matter models, able to better reproduce the power spectrum of structures at galactic scales and below (Bode et al. 2001). All dark matter models however encounter persistent problems at galactic scales, such as the predicted cusps and too high abundance of dark matter in galaxies (e.g. Wang & White 2009, Kennedy et al. 2014, Boylan-Kolchin et al. 2011, 2012).

An alternative to dark matter models which work in Einstein gravity is to assume that a modification of the gravity could account for the apparent dark sector, and in particular the Modified Newtonian Dynamics (MOND) proposed by Milgrom (1983), which is accounting so well for the missing mass at galaxy scales (see the review by Sanders & McGaugh 2002, and Famaey & McGaugh 2012). The fundamental idea is based on the observation that mass discrepancies occur mainly when the acceleration falls below the critical value of $a_0 \sim 2 \cdot 10^{-10} \text{ m/s}^2$. At low acceleration, the gravitational force is varying as $1/r$ instead of $1/r^2$. Outer parts of giant galaxies, and dwarf galaxies should fall entirely in this regime.

In standard dark matter models, bulges in galaxies are thought to be formed mainly through major or minor mergers (e.g. Toomre 1977, Barnes & Hernquist 1991, Naab & Burkert 2003, Bournaud et al. 2005, 2007a). The time-scale of a merger

is short, of the order of 10% of the Hubble time or less, because of the existence of extended and massive dark halos, which take the orbital angular momentum of baryons away (Barnes 1988). In modified gravity models, in the absence of halos, the spiral-in of companion galaxies occur on a much larger time-scale, and the frequency of mergers is low (Tiret & Combes 2008b). The prediction of the number and mass of bulges in spiral galaxies could then be a discriminant between models. Another way to form bulges occur in the early universe, when gas-rich disks are unstable to collapsing into massive clumps, which spiral-in and form a bulge and thick disk (e.g. Noguchi 1999, Bournaud et al. 2007b). Dynamical friction is thought to bring the clumps inwards, faster than their destruction through star formation feedback, and this could also constrain dark matter models.

There is also a third main dynamical process able to form bulges in spiral galaxies, the vertical resonance with a stellar bar (Combes et al. 1990, Kormendy & Kennicutt 2004). These are called pseudo-bulges, since they show more rotation, more flattening, and a radial distribution closer to an exponential than "classical" bulges. Bars are forming at comparable frequency in MOND and Newtonian models with dark matter (Tiret & Combes, 2007, 2008a), and pseudo-bulges are expected to form as frequently in the two models.

The scope of the present article is to compare the formation of bulges in clumpy disks in the frame of dark matter and MOND models, to probe early bulge formation. The methods for the simulations are described in Section 2, and the galaxy models used in Section 3. The results are first presented for dynamical friction in dissipation-less models (Section 4.1), and then the full phenomena of gas-rich disks forming clumpy galaxies, with star formation and feedback are included in Section 4.2, and discussed in Section 5. The conclusions of bulge formation in the different models are then summarised in Section 6.

Send offprint requests to: F. Combes

2. Simulation methods

Since the MOND equations are non linear, it is not possible to use normal Poisson solvers, such as the Tree code, but instead the full differential equations should be solved on a grid. This is very efficiently done with the multigrid algorithm (cf Numerical Recipes, Press et al., 1992, Brada & Milgrom 1999, Tiret & Combes 2007, hereafter TC07). Both the MOND simulations, and the Newtonian gravity comparison runs were carried out with the same multigrid method. For the modified gravity runs, the self-consistent Lagrangian theory AQUAL, developed by Bekenstein & Milgrom (1984) was used, where the Poisson equation is written as:

$$\nabla[\mu(|\nabla\Phi|/a_0)\nabla\Phi] = 4\pi G\rho, \quad (1)$$

where $\mu(x)$ is the interpolation function that is equal to unity at large x (Newtonian regime), and tends to x when $x \ll 1$ in the MOND regime. Various functions have been used in the literature, and for fitting rotation curves of spiral galaxies the best one appears to be the standard function $\mu(x) = x/(1+x^2)^{1/2}$ (Sanders & McGaugh 2002), while for the Milky Way the best fit is obtained with the so-called "simple" function $\mu(x) = x/(1+x)$ (Famaey & Binney 2005). The values of a_0 range between 1 and $2 \cdot 10^{-10} \text{ m/s}^2$, according to the μ function used: with the simple function, the MOND regime is reached with an acceleration about one order of magnitude larger than with the standard function (e.g. Tiret & Combes 2008a). There are other uncertain parameters that could influence the choice of the coupled parameters (μ , a_0) as for instance the unknown fraction of dark baryons in galaxy disks (Tiret & Combes 2009), or the impact of the external field effect (Zhao & Famaey 2006).

The multigrid method developed in the present work has been described at length and tested in TC07, and in particular the problem of boundary conditions. The equation (1) has been discretized similarly, and the Gauss-Seidel relaxation with red and black ordering was followed. If the convergence is very quick with the linear Newtonian Poisson equation, the analogous MOND equations take a much longer CPU time. Then to be able to run many more simulations in a given time, I used the quasi linear formulation of MOND, call QUMOND developed by Milgrom (2010).

This formulation has the advantage to be much easier to solve, since the interpolation function of a/a_0 has been transferred to its inverse equivalent, as a function of a_N/a_0 , a_N being the Newtonian acceleration. It is a non-relativistic complete theory, derivable from an action, but the non linearity can be reduced to solve several times the linear Poisson equation. Indeed the equation to solve is the following:

$$\nabla^2\Phi = \nabla[v(|\nabla\Phi_N|/a_0)\nabla\Phi_N] \quad (2)$$

where Φ is the Milgromian potential and Φ_N the Newtonian one. Since the normal Poisson equation links Φ_N and the density ρ by the relation $\nabla^2\Phi_N = 4\pi G\rho$, equation (2) can be written as the function of two densities:

$$\nabla^2\Phi = 4\pi G\rho_b + 4\pi G\rho_{ph}$$

where ρ_b is the baryonic density, and ρ_{ph} the so-called phantom density, which is the equivalent of the missing mass within the Newtonian gravity. Examples of the phantom density distribution are given by Lüghausen et al. (2013), it can sometimes (rarely) be negative. The phantom density can be computed by

$$\rho_{ph} = \frac{1}{4\pi G} \nabla[(v-1)\nabla\Phi_N] \quad (3)$$

The computation of the Milgromian potential therefore can be carried out in two linear steps. First the Newtonian potential Φ_N is computed on the grid from the baryonic density ρ_b , and the phantom density ρ_{ph} is derived on the same grid, through discretisation of equation (3), (see, e.g. Famaey & McGaugh 2012), in a similar manner as for equation (1). Then the linear Newtonian Poisson solver is used again, this time with $\rho_b + \rho_{ph}$. The interpolation function $v(a_N/a_0)$ corresponding to the standard μ function can easily be computed as $v(y) = \sqrt{0.5 + 0.5\sqrt{1 + 4/y^2}}$. The two MOND formulations AQUAL and QUMOND are not completely equivalent, since their forces differ by a curl field (Zhao & Famaey 2010). The two are very close in symmetric systems however, and in what follows, the results obtained from the two formulations were checked to be similar.

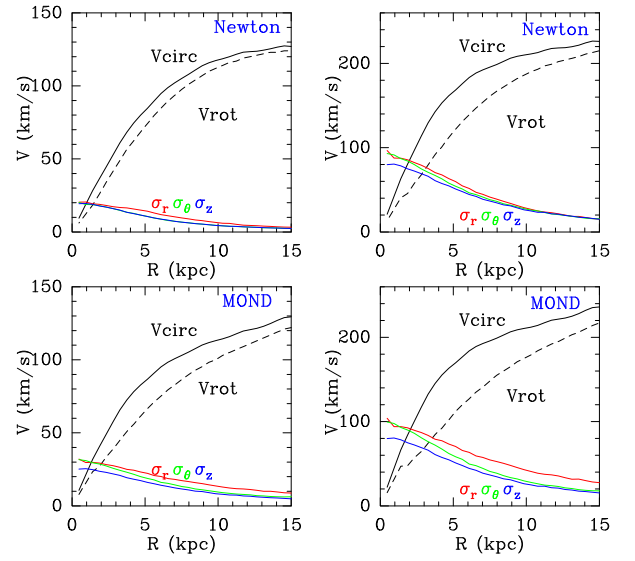


Fig. 1. Left: Circular and rotational velocities, together with the velocity dispersions for the stellar component in the Newtonian +DM (top) and MOND (bottom) initial galaxy models with stars and gas. Right: Same for the giant galaxy model.

The grid used in the present work is 257^3 in size. The simulation box covers a 60 kpc cube, the spatial resolution is about 230 pc. The rest of the simulation code works like a particle-mesh (PM) code. Up to 0.75 million particles are distributed initially on the grid. The density is computed on the grid by a cloud-in-cell (CIC) algorithm, and once the potential is computed, particles are advanced using a leap-frog method. For the purpose of discriminating the various physical mechanisms, simulations with only stars (and dark matter in the Newtonian equivalent systems) have been run, and then later simulations including gas, star formation and feedback. The gas dissipation has been taken into account with a sticky-particle code, as described in Tiret & Combes (2008a). The rebound parameters have been varied from 0.4 to 1, which impacted essentially the amount of dissipation, and the time-scales of clump formation. The runs presented in the following are all with $\beta_r = \beta_i = 0.5$. The variety of results obtained with a changing gas dissipation does not change fundamentally the conclusions.

Star formation follows a Schmidt law, i.e. the star formation rate (SFR) is proportional to a power n of the local volumic den-

sity, with a density threshold. The exponent n has been taken equal to 1.4 (Kennicutt 1998). This non-linear relation means that gas clumps will be preferentially the site of star formation. The proportionality factor is selected to give a depletion time-scale for an homogeneous gas disk of 5 Gyr, in its initial state. When clumps form, the consumption time-scale is considerably reduced, due to the higher star formation efficiency in dense clumps. A continuous mass loss from stars into the gas is taken into account as in Jungwiert et al (2001). The mass loss by stars is distributed through the gas on neighbouring particles, with a velocity dispersion, to schematize the feedback energy.

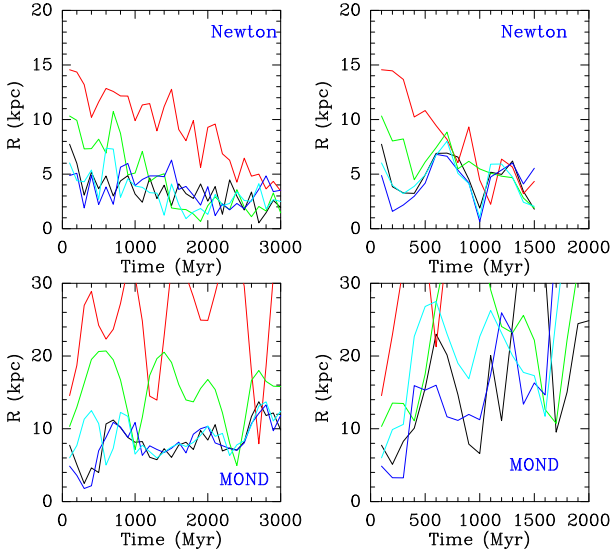


Fig. 2. **Left:** Decay of the 5 clumps containing globally 25% of the baryonic disk as a function of time, in the Newtonian +DM (top) and MOND (bottom), for the purely stellar galaxy models. **Right:** Same for the giant galaxy model.

3. The model galaxies

The goal of the present work is to study the formation of bulges in the early universe, therefore the initial conditions are gas-rich galaxies, with a gas fraction of 50% of the baryonic mass, with no bulge to start with.

The stellar disk follows a Miyamoto-Nagai density profile:

$$\rho_*(R, z) = \left(\frac{h z_*^2 M_*}{4\pi} \right) \times \frac{hr_* R^2 + (hr_* + 3\sqrt{z^2 + h z_*^2}) \left(hr_* + \sqrt{z^2 + h z_*^2} \right)^2}{\left[R^2 + \left(hr_* + \sqrt{z^2 + h z_*^2} \right)^2 \right]^{5/2} (z^2 + h z_*^2)^{3/2}} \quad (4)$$

with a mass M_* and radial and vertical scale lengths hr_* and $h z_*$, respectively. The gas disk follows the same distribution, with characteristic parameters M_g , hr_g and $h z_g$, respectively. All values of parameters are displayed in Table 1. The simulation resolution (230 pc) is barely enough to study the vertical structure

Table 2. Estimate of decay time-scales

| Model | 5 clumps ⁽¹⁾ | 3 clumps ⁽²⁾ |
|-------|-------------------------|-------------------------|
| dwarf | 1.4 ± 0.2 | 0.7 ± 0.12 |
| giant | 0.5 ± 0.07 | 0.2 ± 0.04 |

⁽¹⁾ Each clump has a mass of 5% of the baryonic mass

⁽²⁾ Each clump has a mass of 10% of the baryonic mass

Decay time-scales are in Gyr

of the gas disk (500 pc). All components are truncated at 3 times the value of their characteristic scale, therefore the extent of the disk is initially 15 kpc in radius.

In the equivalent Newtonian galaxies, the dark halo is modelled as a Plummer sphere, with characteristic mass M_H and characteristic radius R_H . Its density is given by the following analytical formula:

$$\rho_H(r) = \left(\frac{3M_H}{4\pi R_H^3} \right) \left(1 + \frac{r^2}{R_H^2} \right)^{-5/2} \quad (5)$$

The values of these parameters M_H and hr_H are selected so that the Newtonian equivalent model has the same rotation curve as the disk in the modified dynamics. The dark matter halo is truncated at 21 kpc, and halo masses indicated in Table 1 are relevant to this radius.

The stability of these galaxy models is controlled initially through a Toomre parameter for the stellar disk of $Q_{\text{star}} = 1.5$, and for the gas component, $Q_{\text{gas}} = 1.1$. The initial rotation curves of the model galaxies are shown in Fig.1. To avoid artificial initial relaxation of the disks, particles are advanced during a typical rotation period in the frozen initial potential, computed with the multi-grid potential solver. No gas dissipation, nor star formation are included in this relaxation phase.

4. Results

To isolate the main physical parameters, purely stellar models are run first, although they do not correspond to the reality of galaxies in the early universe. They will be compared to analogous simulations, where half of the baryonic mass is gas. This will emphasize the role of dissipation, star formation and feedback.

4.1. Dissipationless models

Two extreme mass models, dwarf and giant galaxies, were run with the same characteristic scales, but with masses different by an order of magnitude (see Table 1). To quantify the effects of dynamical friction, initial clumps were simulated by massive particles, in two options: either 5 clumps containing globally 25% of the disk mass; or 3 clumps containing 30% of the disk mass were distributed randomly, with the same initial velocity distribution as the rest of particles. In total, 8 types of run were carried out, with two mass models, two types of clumps, and for the two gravity models. For each type of run, 10 different random realisations of the initial conditions were used, to average out the results. The decay of the clumps through dynamical friction is illustrated in some of these runs in Figure 2. An estimate of the decay time-scale (time for the clumps to fall from their initial radius to the central region at 1-2kpc where their orbit reaches a stationary state) is obtained through averaging

Table 1. Simulation models

| Model | M_* $10^9 M_\odot$ | h_{r*} kpc | h_{z*} kpc | M_g $10^9 M_\odot$ | h_{rg} kpc | h_{zg} kpc | β_r | β_t | C_{star} | α | $M_H^{(1)}$ $10^{10} M_\odot$ | R_H kpc |
|----------------------|-------------------------|-----------------|-----------------|-------------------------|-----------------|-----------------|-----------|-----------|-------------------|----------|----------------------------------|--------------|
| dwarf ^(*) | 5.68 | 5. | 1. | 0. | - | - | - | - | - | - | 7.5 | 12 |
| dwarf | 2.84 | 5. | 1. | 2.84 | 5. | 0.5 | 0.5 | 0.5 | $2 \cdot 10^{-4}$ | 1.4 | 7.5 | 12 |
| giant ^(*) | 56.8 | 5. | 1. | 0. | - | - | - | - | - | - | 17.6 | 16 |
| giant | 28.4 | 5. | 1. | 28.4 | 5. | 0.5 | 0.5 | 0.5 | $2 \cdot 10^{-4}$ | 1.4 | 17.6 | 16 |

^(*) These runs are purely stellar

⁽¹⁾ Dark halo mass of the equivalent Newtonian system

The depletion time-scale is 5 Gyr, for the homogeneous gas disk

of these clump orbits, and is gathered in Table 2. All realisations of a given run type are averaged out, and all orbits which are selected randomly. This procedure looks more realistic than launching a given clump alone at an external radius, since the dynamical effects of all the clumps interfere in the deformations impacted on the dark halo and other particles in the disk. This interference of several clumps can reduce and sometimes increase the dynamical friction effect (Weinberg 1989). Also the decay time-scales depend on the launching radius, and in the same run, the clumps starting at smaller radii have a smaller decay time-scale. Although these final averaged values have relative error bars of 10-20%, they are compatible in their mass and density dependency with the Chandrasekhar formula for dynamical friction (Chandrasekhar 1943). The decay time is predicted to be inversely proportional to the clump mass, for a given background distribution, and with the present assumptions on radii and mass ratios between clumps and disk, roughly inversely proportional to the square root of the total host mass. It is only an approximation of course, since many other parameters enter into account, as the initial velocity of the clump, the dark and baryonic radial mass distributions etc. It was not possible to measure the corresponding values in the MOND models, due to weak dynamical friction.

4.2. Models with gas, star formation and feedback

Figures 3, 4 and 6 show the evolution of the gas and total baryonic component of some models with gas. The disks are highly unstable to clump formation due to the high gas fraction of 50% and the absence of bulge. Control runs with only stars were relatively stable, forming however a strong bar, after 500 Myr for the MOND disks and more than 2 Gyr for the Newtonian ones. The mass in clumps increases at the beginning with the gravitational instability due to the gas dissipation and large gas fraction. But these over-dense regions are very efficient to form stars, and the gas fraction in clumps decreases, as well as the global gas fraction. Figure 5 shows the evolution of the star formation rate (SFR) with time, and the corresponding consumption of the gas. Since the SFR law adopted is non linear, the formation of dense clumps leads to intense starbursts with an episodic character, which consume the gas much quicker than the analogous quiescent, almost homogeneous disk galaxy, which was used as a calibrator of depletion time.

In the absence of external gas accretion and replenishment of the gas content, the disk becomes less unstable. Both through the star formation feedback, and the gravitational shear on the stellar clumps, the mass fraction in clumps slowly decreases. The dynamical friction due to the dark halo on the clumps is however fast enough to bring the clumps towards the center and build a bulge in the Newtonian runs. In the MOND models, the stellar

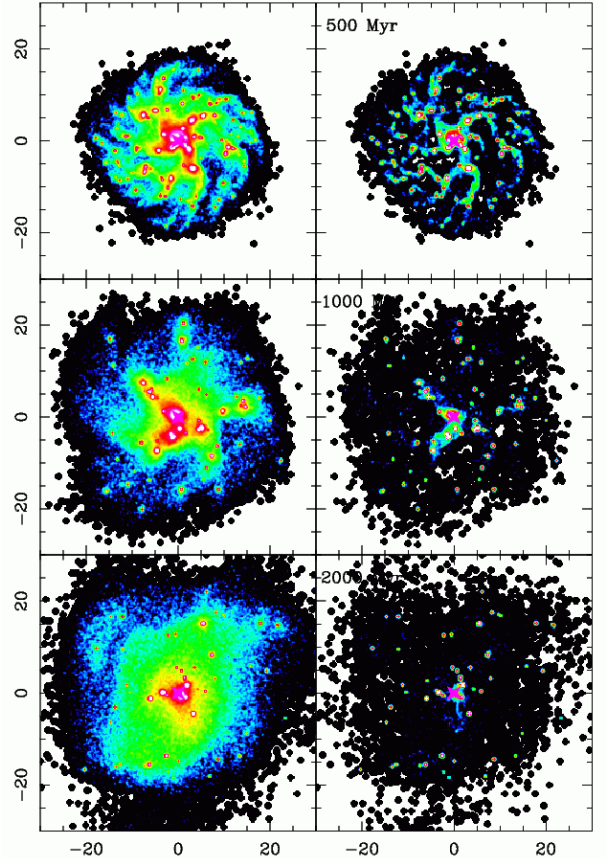


Fig. 3. All baryons (left) and gas (right) surface densities of the dwarf clumpy galaxy, simulated with MOND gravity, at epochs 0.5, 1 and 2 Gyr. Each panel is 60 kpc in size. The color scale is logarithmic and the same for all plots.

fragments are maintained in the disk, because of the weaker dynamical friction from the disk.

The evolution of the stellar surface density Σ as a function of time, is shown in Fig. 7 for the giant galaxy in the Newtonian model, and in Fig. 7 in the MOND gravity. Initially, there is essentially an exponential distribution in the disk, while progressively a second component is accumulated towards the center, in the clumpy galaxy with dark matter. An edge-on view reveals that indeed, there is a small spheroid in the center, together with a thick disk (Fig. 9). This initial bulge formation due to massive clumps has been discussed widely in the literature (Noguchi 1999, Immeli et al. 2004, Bournaud et al. 2007b, Elmegreen et al. 2008), and also the formation of a thick disk from star formation in a turbulent gas disk (Bournaud et al. 2009). Now it is shown that this rapid and early bulge formation does not occur in the

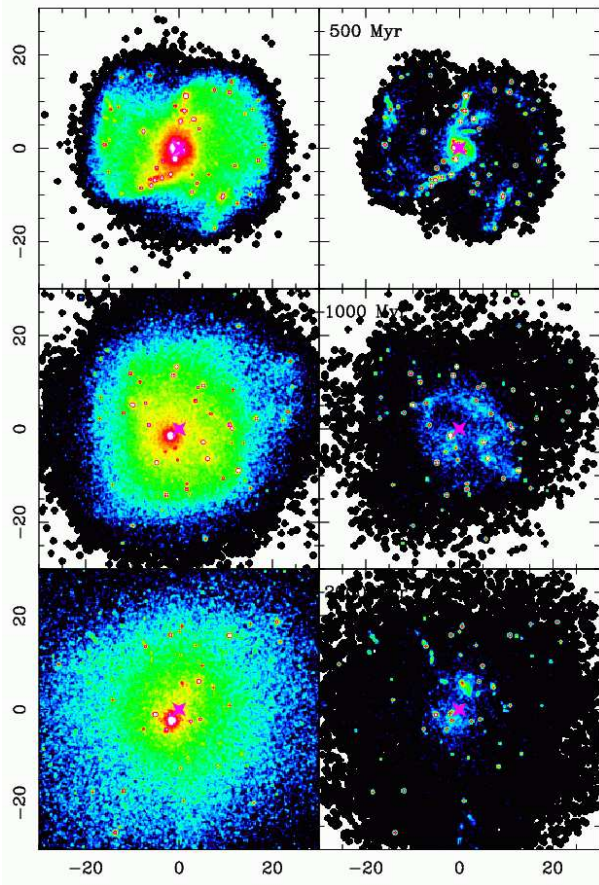


Fig. 4. All baryons (left) and gas (right) surface densities of the giant clumpy galaxy, simulated with MOND gravity, at epochs 0.5, 1 and 2 Gyr. Each panel is 60 kpc in size. The color scale is logarithmic and the same for all plots.

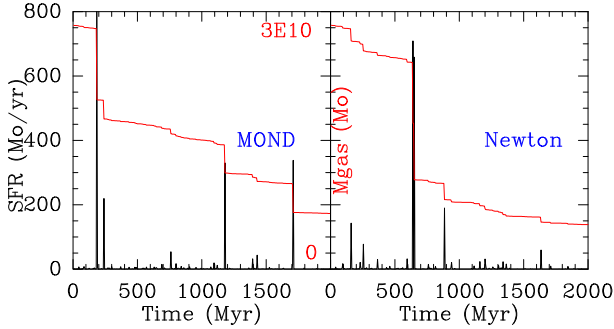


Fig. 5. Evolution of the star formation rate (black line, left scale) and the remaining amount of gas (red lines and middle scale) in the giant galaxy, with MOND (left), and Newtonian dynamics (right).

MOND gravity model. The disk remains clumpy until 2 Gyr, as revealed by Fig. 7. This is the natural consequence of a much longer dynamical friction time-scale.

The mass fraction in clumps was monitored as a function of time, in the same manner as described by Bournaud et al. (2007b). The surface density of the baryonic component is computed at each snapshot. It is first smoothed at a resolution of 700 pc to reduce noise, and the azimuthal average surface density $\Sigma(r)$ is computed at each radius. When the local surface density is

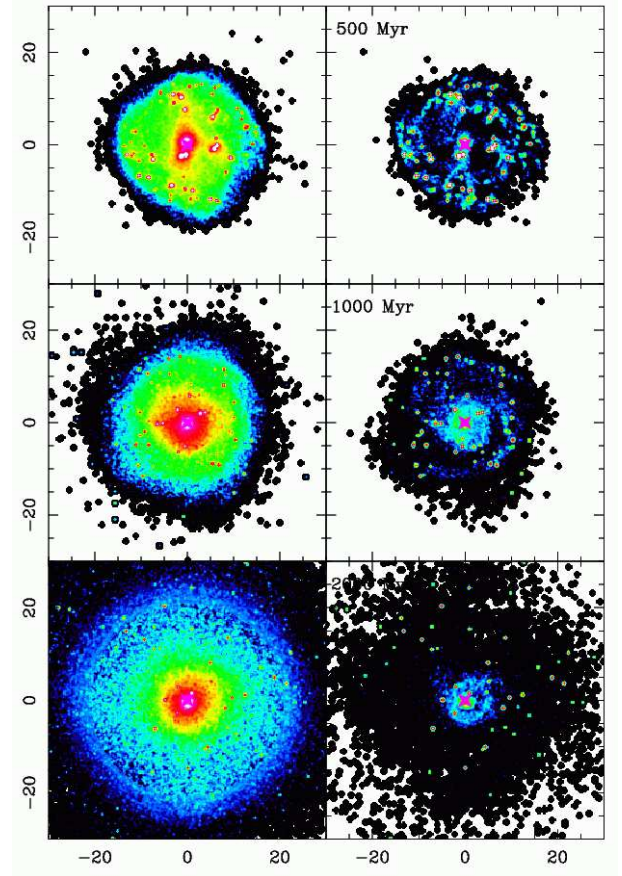


Fig. 6. All baryons (left) and gas (right) surface densities of the giant clumpy galaxy, simulated with Newtonian+DM gravity, at epochs 0.5, 1 and 2 Gyr. Each panel is 60 kpc in size. The color scale is logarithmic and the same for all plots.

higher than 3 times $\Sigma(r)$, it is considered to belong to a clump. When plotted together, these regions do correspond to the main clumps seen in the maps. There is no ambiguity with spiral arms, since the clumps are dominating the global spiral structure (see Fig. 3). The number of clumps found by this method, is typically 10-20. The fraction of the disk mass in clumps can reach at the maximum of the starburst of the order of 30%. Fig. 10 displays the clump mass fraction evolution for the giant model galaxy. It is remarkable that in the MOND regime, the disk galaxy remains highly clumpy, while in the Newtonian gravity with a massive dark matter halo, the clumps are driven toward the center, and the disk becomes more homogeneous, after some last starbursts have consumed the remaining gas.

4.3. Dynamical friction

The different dynamical friction efficiency in the two gravity models is the key to understand the morphology of clumpy galaxies in the early universe, and the bulge formation. The main phenomenon at the origin of the drag on the clumps is the deformation or wake that a massive body imprints on the background distribution of particles. When the bodies have a small mass with respect to the total system, their wake is a small perturbation, and the process can be handled analytically. However, with massive bodies, the true effect of the friction is not intuitive to derive, especially when the massive bodies are numerous, and their wakes interfere. They can perturb the system sig-

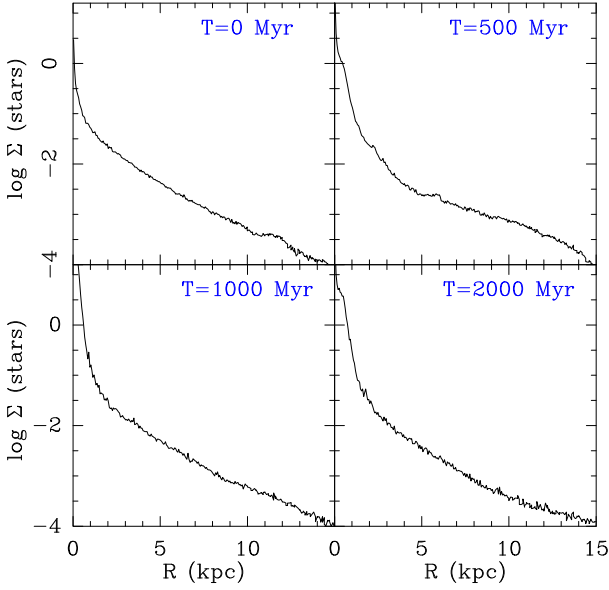


Fig. 7. Stellar profile of the giant galaxy in the Newtonian dynamics, at various epochs (0, 0.5, 1 and 2 Gyr). A bulge is building aside the exponential disk.

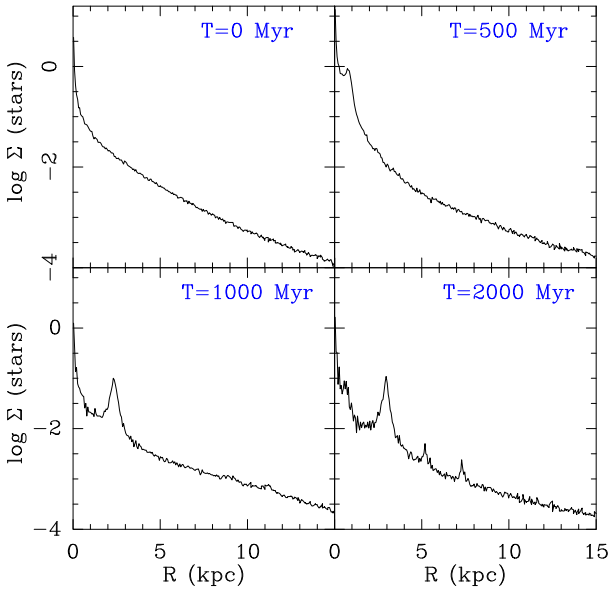


Fig. 8. Same as Fig. 7 for the MOND model.

nificantly, so that it cannot be considered as an infinite reservoir of energy and angular momentum. Results that may look controversial at first sight have been claimed in the literature. Ciotti & Binney (2004) concluded that dynamical friction is stronger in MOND from a perturbation study. They consider only very small-mass bodies, like star clusters, with negligible effect on the global stellar background, and adopt impulse approximation for deflection or orbits and linear summation of effects. On the other side, for the Newtonian model with dark matter, they consider the dark matter halo as a rigid background, not participating in the dynamical friction. They find that the two-body relaxation time is shorter for disks in the MOND regime, and extrapolate these results to the dynamical friction time, obtained for test particles in the local formula of Chandrasekhar (1943).

The consequences would be that globular clusters should spiral inwards to the center in dwarf galaxies in a few dynamical time-scales, as well as galaxies in groups and in clusters. Simulations by Nipoti et al. (2008) confirmed these findings, in the context of tiny perturbations: the massive bodies subject to the friction, either globular clusters or a rigid bar, have to contain less than 5% of the baryonic mass, so that particles in the stellar background absorbing the energy and angular momentum are not globally perturbed. In realistic systems though, Nipoti et al. (2007) found that the merging timescales for spherical systems are significantly longer in MOND than in Newtonian gravity with dark matter, and Tiret & Combes (2007) found that bars keep their pattern speed constant in MOND, while they are strongly slowed down in the Newtonian equivalent system with a dark matter halo. The main conclusion of these apparently different claims is that the dynamical friction time-scale is larger in MOND for satellite galaxy interactions and for stellar bars, since galaxies are not embedded in extended and massive spheroids of dark matter particles, able to accept the orbital angular momentum. Although the impact of very small fluctuations could be larger in MOND than in Newtonian dynamics, the effect saturates quickly when the perturbation is no longer infinitesimal. On the contrary the equivalent Newtonian system with dark matter has shorter dynamical time-scales, and common satellites and bars are slowed down in a few rotation times. The present results extend these conclusions for clumpy galaxies, typical of high redshift systems, where the total clump mass fraction can reach up to 30% of the disk mass, with individual clumps of 10^8 - $10^9 M_\odot$. The typical time-scale for the clumps to be driven to the center and form the bulge in the Newtonian model with dark matter is about 1 Gyr for the giant galaxy, and 3 Gyr for the dwarf. For the MOND model, the dynamical friction is not efficient to form a bulge before the clumps are destroyed or reduced by the star formation feedback and the tidal and shear forces.

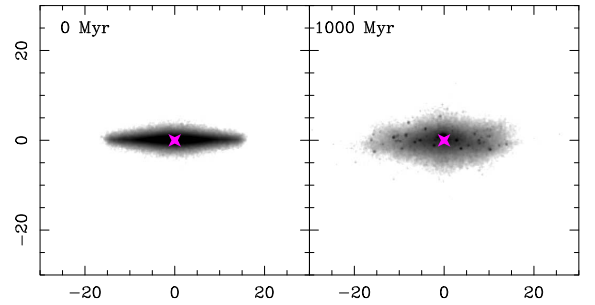


Fig. 9. Evolution of the edge-on morphology of the giant galaxy, in the Newtonian gravity model with gas and star formation.

5. Discussion

The present simulations are based on the simple model of sticky particles for the gas physics and dissipative character. Previous works have used different methods, either sticky-particles (Noguchi 1999, Immeli et al 2004, Bournaud et al 2007a, Elmegreen et al 2008), or AMR hydro-code (Dekel et al 2009, Ceverino et al. 2010, Behrendt et al. 2014) or Tree-SPH code (Hopkins et al. 2012). The results are very similar, as far as the instability of the early galaxies are concerned. Massive clumps are formed, reproducing clumpy galaxies at high red-

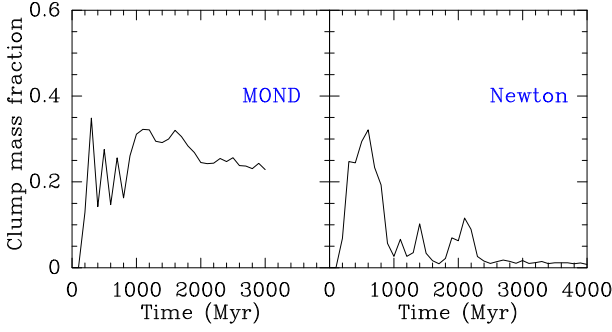


Fig. 10. Evolution of the clump mass fraction (see text for the definition) for the giant galaxy, in the MOND gravity (left) and in the Newtonian gravity (right).

shift. The importance of the bulge formation is variable according to the stellar feedback adopted. Clumps are driven to the center through dynamical friction in less than 1 Gyr for massive galaxies of $\sim 7 \cdot 10^{10} M_{\odot}$ in baryons, but extreme SN feedback could reduce significantly the mass of clumps ending in the bulge (Hopkins et al. 2012). The bulge in all cases has a stabilising influence on the disk, and after the clumpy phase, the disk remains quite homogeneous, even in the case of abundant external gas accretion (Ceverino et al 2010). In the present work, several degrees of dissipation have been tried, and the variation of the collisional parameters β between 0.3 and 0.7 had not a large influence on the results, confirming the conclusions of Bournaud et al. (2007a). The essential point is to have sufficient dissipation in the gas to allow its collapse into dense clumps, and to enhance the star formation rate through a non-linear Schmidt law.

It is also necessary to check that the spatial resolution of the simulations is not perturbing the main conclusions. The 257^3 grid means a resolution of 230 pc for the potential solver, it is always lower than the Jeans scales. From initial conditions, it is possible to predict the range of sizes and masses of clumps in the unstable disks (but see Behrendt et al. 2014). The Jeans length in an axisymmetric disk is $\lambda_J = \sigma_g^2 / (G\Sigma)$, where σ_g is the gas velocity dispersion, and Σ is the disk surface density. These ranges from 0.5 to 1 kpc in the dwarf galaxy model, and from 1.4 to 2 kpc for the giant. The corresponding range in mass of the clumps are $M_J = \pi \sigma_g^4 / (G^2 \Sigma)$, between 10^6 - $10^8 M_{\odot}$ for the dwarf galaxy and 10^8 - $10^9 M_{\odot}$ for the giant model. A higher resolution simulation with 513^3 grid has been run for the dwarf galaxy model, increasing the number of particles to 6 million particles. The clump mass fraction is plotted in Fig. 11. Globally, the evolution is similar, with the clump fraction determined with the smoothing length adapted to the factor 2 higher spatial resolution.

Another interesting issue is the stability of the considered disks to large-scale waves, although the small-scale fragmentation is dominant. The critical wavelength λ_{crit} above which disks should be stabilised by differential rotation, even without pressure (dispersion) terms, indicating the self-gravity scale is $\lambda_{crit} = 4\pi^2 G \Sigma / \kappa$, where κ is the epicyclic frequency. It is ranging from 1-3 kpc in the dwarf galaxy, and 2-6 kpc for the giant. The role of the dark matter halo is proportionally much higher in the dwarf. The X-Toomre parameter, $X = \lambda / \lambda_{crit}$, where $\lambda \sim 2\pi r$, controls the self-gravitating response of the disk, through the swing amplifier; waves develop more efficiently when $X \sim 2$ (Toomre 1981). In the present galaxy models, there exists always a central region where $X \sim 1$ -2.

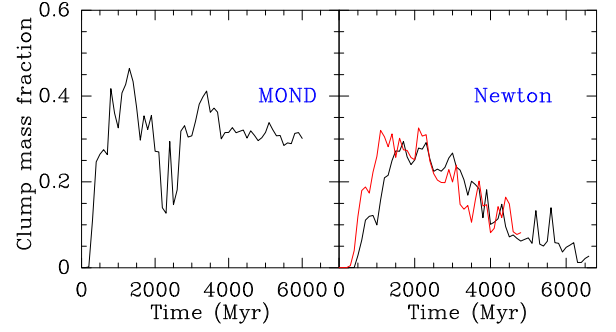


Fig. 11. Evolution of the clump mass fraction for the dwarf galaxy, in the MOND gravity (left) and in the Newtonian gravity (right). The high-resolution run with a 513^3 grid and 8 times the number of particles is plotted in red.

6. Summary

Simulations have been carried out of the dynamical processes occurring early in the universe, in galaxies very rich in gas, and corresponding to the clumpy galaxies observed at high redshift (e.g. Elmegreen & Elmegreen 2005, Elmegreen 2007). Previous works have established that bulge formation is rapid in those galaxies, through dynamical friction driving the clumps to coalesce in the galaxy centers (Noguchi 1999, Bournaud et al. 2007b, Elmegreen et al 2008). The present work explores the analogous phenomena in modified gravity (MOND, Milgrom 1983). A multi-grid code is used to solve the non-linear equations, both from the original AQUAL Lagrangian (Bekenstein & Milgrom 1984), and the QUMOND solution, recently developed by Milgrom (2010). Both appear to give similar results, and most runs were performed in the faster method of QUMOND. For each galaxy model, the corresponding rotation curve is first computed in MOND, and then an equivalent Newtonian system is built, with a dark matter halo added, in order to get exactly the same rotation curve, as in Tirit & Combes (2007, 2008a). The efficiency of dynamical friction was first compared between the two gravity models, with academic purely stellar runs, where an ensemble of clumps were randomly distributed initially with 20-30% of the baryonic mass. A series of such simulations show that clumps should spiral inwards to the center in the Newtonian galaxies in about 1 Gyr or less, while the clumps remain orbiting in the disk for more than 2-3 Gyr in the MOND regime.

The most realistic simulations include gas dissipation, star formation and feedback. Disks are composed initially of 50% of stars and 50% of gas. Rapid fragmentation occurs in these unstable disks, and clumpy galaxies similar to what is observed at high redshift are formed, in both gravity models. This clumpy morphology lasts less than 1 Gyr in the giant galaxy model, of baryonic mass $5.7 \cdot 10^{10} M_{\odot}$, and 3 Gyr in the dwarf galaxy, with 10 times less mass. Clumps are driven inwards by dynamical friction, and form a spheroidal bulge. This is quite compatible to previous works. However, in the MOND gravity model, the clumps remain in the disk during a much longer time-scale, and are eventually destroyed or reduced by stellar feedback and shear, and have no time to fall in the center to form a bulge. The lower bulge formation efficiency in MOND is more in line with the large number of observed bulge-less galaxies today (Kormendy et al. 2010). The latter are difficult to explain in the standard Newton plus dark matter models. Weinzirl et al (2009) compare the observations of the bulge mass and frequency in present-day galaxies, with the predictions of the CDM model.

Massive galaxies can have less than 20% of their baryonic mass in a bulge if they experience mergers only before $z=4$. But galaxies having later mergers and larger bulge fraction are about 30 times more abundant in CDM simulations than observed.

In the frame of MOND, bulges are hardly formed in early times, in the clumpy phase of galaxy formation, when gas is dominating the surface density of galaxy disks. They can form later, through hierarchical merging, with a frequency which is smaller than what occurs in the analogous Newtonian systems with dark matter. They however form with equivalent frequency through secular evolution, by vertical resonances with bars. It is therefore expected that the frequency of pseudo-bulges is higher in MOND. More quantitative statements will require many more simulations with a cosmological context.

Acknowledgements. The idea of this work came when Eija Laurikainen asked me a review article on bulge formation with MOND. The European Research Council for the Advanced Grant Program Number 267399-Momentum is acknowledged. Most simulations have been run on the cluster provided by this ERC grant.

References

- Barnes, J. E.: 1988, *ApJ* 331, 699
 Barnes, J. E., Hernquist, L. E. 1991, *ApJ* 370, L65
 Behrendt, M., Burkert, A., Scharmann, M.: 2014, *MNRAS*
 Bekenstein J., Milgrom M.: 1984, *ApJ* 286, 7
 Bertone G., Hooper D., Silk J.: 2005, *PhR* 405, 279
 Blumenthal G.R., Faber S.M., Primack, J.R., Rees M.J.: 1984, *Nature* 311, 517
 Bode P., Ostriker J.P., Turok N.: 2001, *ApJ* 556, 93
 Bournaud F., Jog C.J., Combes F.: 2005, *A&A* 437, 69
 Bournaud F., Jog C.J., Combes F.: 2007a, *A&A* 476, 1179
 Bournaud F., Elmegreen B.G., Elmegreen D.M.: 2007b *ApJ* 670, 237
 Bournaud F., Elmegreen B.G., Martig M.: 2009, *ApJ* 707, L1
 Boylan-Kolchin, M., Bullock, J. S., Kaplinghat, M.: 2011, *MNRAS* 415, L40
 Boylan-Kolchin, M., Bullock, J. S., Kaplinghat, M.: 2012, *MNRAS* 422, 1203
 Brada R., Milgrom M.: 1999, *ApJ* 519, 590
 Ceverino D., Dekel A., Bournaud F.: 2010, *MNRAS* 404, 2151
 Chandrasekhar S., 1943, *ApJ* 97, 255
 Ciotti L., Binney J.: 2004, *MNRAS* 351, 285
 Combes F., Debbasch F., Friedli D., Pfenniger D.: 1990, *A&A* 233, 82
 Dekel A., Sari R., Ceverino D.: 2009, *ApJ* 703, 785
 Elmegreen B.G., Elmegreen D.M.: 2005, *ApJ* 627, 632
 Elmegreen D.M.: 2007, in *IAU S235*, ed. F. Combes & J. Palous, CUP, p. 376
 Elmegreen B.G., Bournaud F., Elmegreen D.M.: 2008, *ApJ* 688, 67
 Famaey B., Binney J.: 2005, *MNRAS* 363, 603
 Famaey B., McGaugh S. S.: 2012, *Living Reviews in Relativity*, vol. 15, no. 10
 Hopkins, P. F., Keres, D., Murray, N. et al.: 2012, *MNRAS* 427, 968
 Immeli A., Samland M., Gerhard O., Westera P.: 2004, *A&A* 413, 547
 Jungwiert B., Combes F., Palous J.: 2001, *A&A* 376, 85
 Kennedy R., Frenk C., Cole S., Benson A.: 2014, *MNRAS* 442, 2487
 Kennicutt R.C.: 1998, *ApJ* 498, 541
 Kormendy, J., Kennicutt, R. C.: 2004, *ARAA* 42, 603
 Kormendy J., Drory N., Bender R., Cornell M. E., 2010, *ApJ* 723, 54
 Lüghausen F., Famaey B., Kroupa P. et al.: 2013, *MNRAS* 432, 2846
 Milgrom M.: 1983, *ApJ* 270, 365
 Milgrom M.: 2010 *MNRAS* 403, 886
 Naab, T., Burkert, A. 2003, *ApJ* 597, 893
 Nipoti, C., Londrillo, P., Ciotti, L., 2007, *MNRAS* 381, 104
 Nipoti, C., Ciotti, L., Binney, J., Londrillo, P.: 2008, *MNRAS* 386, 2194
 Noguchi M.: 1999, *ApJ* 514, 77
 Peebles P.J.E., Ratra B.: 2003, *RvMP* 75, 559
 Press W.H., Teukolsky S.A., Vetterling W.T., Flannery B.P., *Numerical Recipes in Fortran 77*, second edition, Cambridge University Press, 1992
 Sanders R.H., McGaugh S.: 2002, *ARAA* 40, 263
 Tirit O., Combes F.: 2007, *A&A* 464, 517
 Tirit O., Combes F.: 2008a, *A&A* 483, 719
 Tirit O., Combes F.: 2008b *ASPC* 396, 259
 Tirit O., Combes F.: 2009, *A&A* 496, 659
 Toomre A.: 1977, in *Evolution of Galaxies and Stellar Populations*, Proceedings of a Conference at Yale University, p. 401
 Toomre A.: 1981, *Proceedings of the Advanced Study Institute*, Cambridge, England, CUP p.111-136
 Wang J., White S.D.M.: 2009, *MNRAS* 396, 709
 Weinberg, M.D.: 1989, *MNRAS* 239, 549
 Weinzirl T., Jogee S., Khochfar S. et al.: 2009, *ApJ* 696, 411
 Zhao, H.S., Famaey, B.: 2006, *ApJ* 638, L9
 Zhao, H.S., Famaey, B.: 2010, *Phys. Rev. D*, 81(8), 087304